

Controlling and characterizing Floquet prethermalization in a driven quantum system

K. Singh^{1*}, K. M. Fujiwara^{1*}, Z. A. Geiger¹, E. Q. Simmons¹, M. Lipatov¹,
 A. Cao¹, P. Dotti¹, S. V. Rajagopal¹, R. Senaratne¹, T. Shimasaki¹,
 M. Heyl², A. Eckardt², and D. M. Weld^{1†}

¹Department of Physics, University of California, Santa Barbara, California 93106, USA

²Max-Planck-Institut für Physik komplexer Systeme, Nöthnitzer Str. 38, 01187 Dresden, Germany

* Equal contributions.

†To whom correspondence should be addressed; E-mail: weld@ucsb.edu.

Periodic driving is a powerful tool for engineering tunable many-body quantum states. Such Floquet engineering relies on the existence of a localized prethermal regime, a state which remains incompletely understood. We report experiments on a many-body Floquet system consisting of ultracold atoms in an optical lattice subjected to sign-changing amplitude modulation. A double-quench protocol enables measurement of an inverse participation ratio quantifying the degree of prethermal localization as a function of continuously tunable drive parameters and interactions. Following the time evolution of the driven system, we observe the sequential formation of two localized prethermal plateaux, interaction-driven delocalization, and strongly frequency-dependent dynamics of departure from the prethermal state. The experimental control and quantitative characterization of Floquet prethermalization opens new possibilities for dynamical quantum engineering.

Floquet engineering has emerged as a powerful technique for building novel quantum states with drive-dependent properties (1–11). While interacting driven multi-band systems are generally expected to heat to infinite temperature at infinite time, this does not preclude the realization of nontrivial states at intermediate (and in certain cases exponentially long) time scales (12–16). For undriven systems, such prethermalization plateaux (17, 18) admit a statistical description in terms of generalized Gibbs ensembles (19–21) and have been observed in experiments (22–24).

Driven systems, by analogy, are theorized to exhibit *Floquet prethermalization* plateaux and quasi-steady states describable by a *periodic* Gibbs ensemble (PGE) (13, 25–29). These PGEs allow computation of physical observables in non-equilibrium periodically driven systems.

We report experiments which explore a new regime of strongly-driven quantum systems, probing the evolution of tunably-interacting ^7Li atoms in an optical lattice amplitude-modulated at up to a thousand percent. A double quench protocol enables measurement of an inverse participation ratio (IPR) quantifying the localization of the initial state in the basis of the Floquet eigenstates of the one-cycle evolution operator. Starting the driven evolution from the undriven ground state, the experimentally measurable time-averaged occupation of this single-particle ground state is equal to the IPR characterizing the localization of the initial undriven state in the basis of Floquet states. Non-zero values of f_0 correspond to a localized prethermal state, while f_0 drops to zero in the ergodic regime. We experimentally map out a Floquet delocalization crossover in the space of drive parameters, and measure characteristics of the prethermal state which are in quantitative agreement with theoretical calculations based on a periodic Gibbs ensemble. Tracking the time evolution of the driven system, we observe the approach to the prethermal plateau as well as the long-time departure from it, either by the formation of a second prethermal plateau or, for stronger interactions, by complete delocalization.

Previous experiments have examined the role of driving on many-body localized systems (30) and on driving near the lattice band gap (31–34). In this work we study multi-band dynamics without disorder in the strongly-modulated regime, choosing modulation frequencies extending from 0.1 to 10 times the lattice band gap. This frequency range represents a particular challenge for theory due to the breakdown of the Floquet-Magnus expansion.

If interactions are tuned to zero, the Hamiltonian describing our system is $H(t) = -(\hbar^2/2m)\partial_x^2 + V_0[1 + \alpha \sin(\omega t)]\cos^2(k_L x)$, where x is position along the lattice, α is the dimensionless modulation amplitude, ω is the modulation frequency, V_0 is the time-averaged lattice depth, m is the atomic mass, and k_L is the wavenumber of the lattice laser ($\lambda = 1064$ nm) with recoil energy $E_R = \hbar^2 k_L^2 / 2m$. The drive frequency can be expressed dimensionlessly as $\Omega = \omega/\omega_0$ where $\omega_0 = 2\sqrt{V_0 E_R}/\hbar$ is the frequency of harmonic motion in a single lattice site, which approximates the lowest band gap of the static lattice. We realize the strongly-modulated regime $\alpha > 1$ by simultaneously modulating two orthogonally-polarized collinear 1D optical lattices with a relative spatial phase shift of $\lambda/4$. Exploration of this strong driving regime is a key experimental novelty of the work we report, and it is required for access to the majority of the parameter space we explore in maps like those of Fig. 1.

We utilize a double-quench protocol to probe the dynamics of the Floquet Hamiltonian. The atoms are initially prepared in the ground band of a static optical lattice of depth $V_0 = 10E_R$ at zero quasimomentum. The system is then quenched into the Floquet Hamiltonian by applying lattice amplitude modulation at some Ω and α . After a fixed amount of modulation time, the

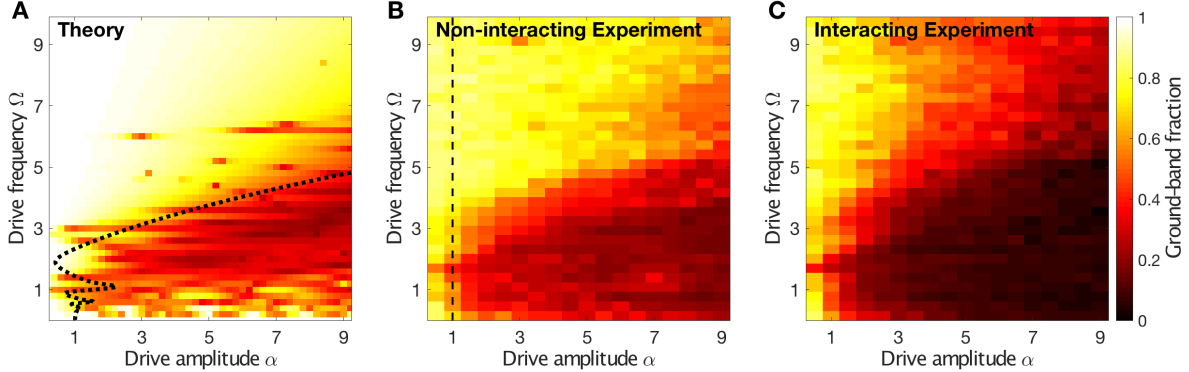


Figure 1: Drive-parameter dependence of Floquet prethermal state. **A:** Theoretical map of the ground band occupation fraction for a periodic Gibbs ensemble. Dashed line shows classical stability boundary of the equivalent driven pendulum. **B:** Experimental measurement of normalized population in the center of the lowest band after a $500 \mu\text{s}$ hold of a non-interacting quantum gas in a modulated optical lattice, as a function of normalized drive frequency Ω and normalized drive amplitude α . The $\alpha > 1$ region to the right of the vertical dashed line is inaccessible without the sign-changing amplitude modulation introduced in this work. **C:** Same measurement as B, but with Feshbach-induced interactions (s -wave scattering length 30 nm). Colorbar is the same for all three panels.

system is quenched back to a static $10E_R$ lattice to perform read-out of the many-body system in the eigenstates of the static optical lattice.

The fraction of atoms remaining in the single-particle ground state after modulation, f_0 , provides a quantitative measure for characterizing localization and non-ergodicity as a function of drive parameters. As shown explicitly in the supplementary material, f_0 corresponds directly to the inverse participation ratio $\sum_n |\langle \psi_0 | n \rangle|^4$ that quantifies the localization of the ground state $|\psi_0\rangle$ in the basis of the Floquet states $|n\rangle$. The theoretically predicted dependence $f_0(\alpha, \Omega)$ obtained from the PGE characterized by integrals of motion given by the occupations $\hat{n}_i(t)$ of the single-particle Floquet modes i is shown in Fig. 1A as a function of dimensionless driving amplitude α and frequency Ω . Figures 1B and 1C show experimentally measured maps of $f_0(\alpha, \Omega)$, for non-interacting and interacting samples respectively. Here the drive is allowed to fully complete the final modulation cycle before band-mapping. Quasimomentum resolution is limited by the finite initial spatial size of the condensate and a finite time-of-flight; the experimental maps are based on integrals over the central 40% of the Brillouin zone. The non-interacting measurement of Fig. 1B shows good agreement with the PGE-based theoretical prediction of Fig. 1A: $f_0 \simeq 1$ for a large region in (α, Ω) space, and as Ω decreases from large values for any given drive amplitude, there is always some alpha-dependent drive frequency below which f_0 sharply decreases to a finite value between 0 and 1. This sharp crossover corresponds approx-

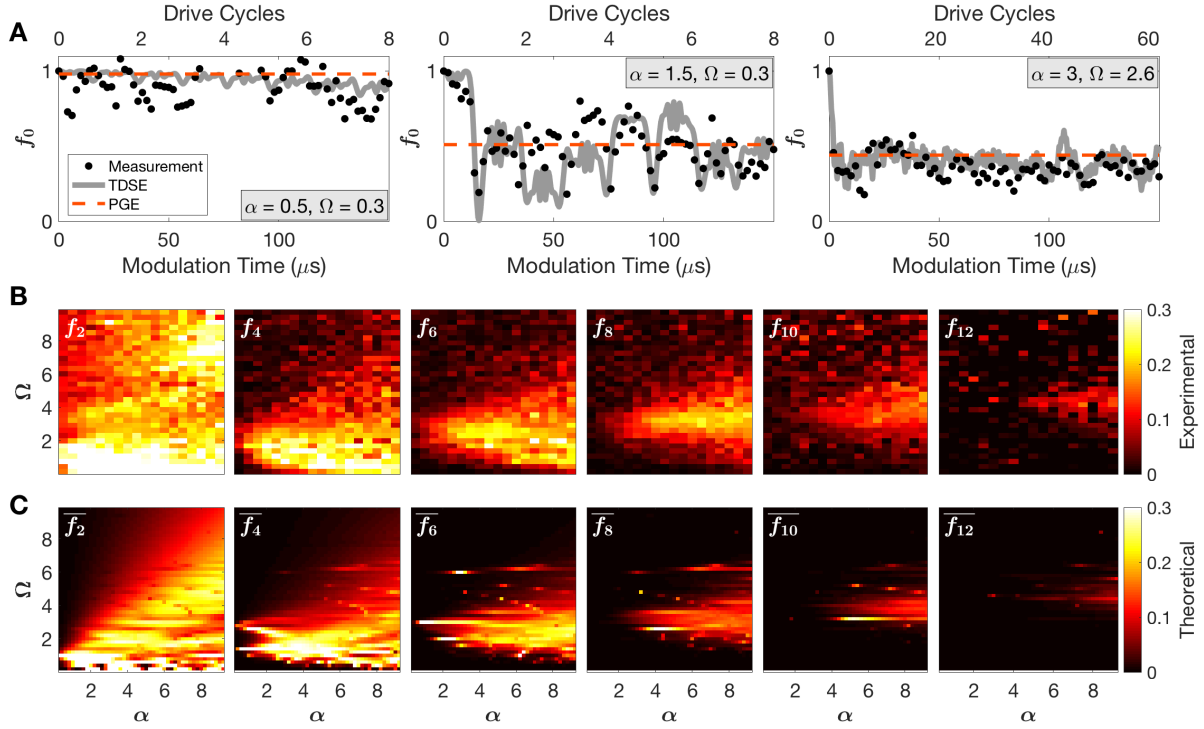


Figure 2: Characterizing the prethermal PGE. **A:** Measured f_0 versus modulation time for the first 150 μ s of the drive, for three different values of (α, Ω) all at $a = 0$. Dashed line shows PGE prediction and solid line shows the results of a time-dependent Schrödinger equation calculation. For these data, the optical lattice is immediately quenched to the initial 10 E_R static lattice at the indicated modulation time and then band-mapped. **B:** Measured atom number fraction in the central 40% of all even excited bands up to the twelfth, as a function of drive parameters α and Ω . **C:** Theoretical prediction of the same quantity in the PGE. All axes and colorbars are the same.

imately to the stable-unstable crossover of the corresponding classical system (dashed line in Fig. 1A). The interacting data in Fig. 1C display a qualitatively similar but not quantitatively identical behavior; the detailed effects of interactions are explored further in the time-evolution measurements discussed below. Mapping out the localization properties of a Floquet system in the regime of ultrastrong driving is the first main result of this report.

As shown in Fig. 2A, the measured time evolution of f_0 for various drive parameters shows rapid attainment of an average value in close agreement with the PGE theoretical prediction, on timescales near a single drive period. Fig. S1 shows that higher-band observables can be used to measure a more gradual entry into the prethermal state, over a few tens of drive periods. For a drive with $\Omega = 0.3$ and $\alpha = 0.5$, f_0 remains close to 1, while for higher drive amplitudes and frequencies it exhibits irregular oscillations near a lower average value in agreement with

the PGE prediction. The oscillations around the mean value are a consequence of the small accessible number of single-particle degrees of freedom in the prethermal state (discussed further in the supplementary material) and are qualitatively consistent with predictions from numerical solutions of the time-dependent Schrödinger equation, also shown in Fig. 2A. The early-time dynamics are not observed to be significantly interaction-dependent; as Fig. 3A shows, both interacting and non-interacting samples attain a similar value of f_0 over the timescales displayed in Fig. 2A.

Measuring higher-band observables in addition to f_0 allows a fuller comparison to theoretical descriptions of the prethermal state. We observe experimentally that over the timescales shown in Fig. 2 the dynamics of the noninteracting driven system mainly redistribute population among the lowest few even Bloch bands, as expected from parity conservation at $k = 0$. The top row of Fig. 2B shows the fractional population of the first six even-parity excited bands measured for each (α, Ω) point, using the same double-quench protocol used to produce Fig. 1. We do not observe significant occupation above the twelfth band, in agreement with the PGE model. The measured band occupations can be directly compared to theory: the bottom row of Fig. 2B shows the theoretically predicted band occupations based on the PGE description, as a function of α and Ω . The close match between theory and experiment provides further support for the PGE description of the prethermal state. These results constitute a direct measurement of the full drive-dependent periodic Gibbs ensemble at each point of drive parameter space.

The long-time evolution of interacting driven systems is both especially relevant for the realization of useful many-body Floquet engineering, and especially challenging to address theoretically. Fig. 3A compares the initial evolution of samples with different interaction strength under the same drive parameters ($\Omega = 2.6$, $\alpha = 3$). For all three values of the interaction strength, the early-time dynamics are in agreement with the PGE description. As the system continues to evolve to large times, the PGE plateau decays. Strikingly, for a wide range of parameters we observe, as shown in Fig. 3B, that the system enters a second plateau in which f_0 is non-zero but smaller than in the first plateau. Non-interacting and weakly-interacting samples remain in this second plateau for at least twenty thousand drive cycles at $\Omega = 2.6$. This second plateau can be understood as a consequence of a slow spreading in quasimomentum: as the modulation proceeds, the initial atomic wavepacket spreads in quasimomentum and the selection rules that prohibit odd band occupation at $k = 0$ are broken. To account for this spreading, all measurements of f_0 in Fig. 3 integrate over the entirety of the first Brillouin zone.

Strongly-interacting samples subjected to the same relatively low-frequency drive do not exhibit this second plateau but instead are observed to attain ergodicity, decaying towards an infinite-temperature state with no detectable atoms in the ground band. However, even for these strongly interacting samples, we observe that the prethermal plateau can be regained by increasing the drive frequency. Figs. 3C-E investigate the long-time evolution of the participation

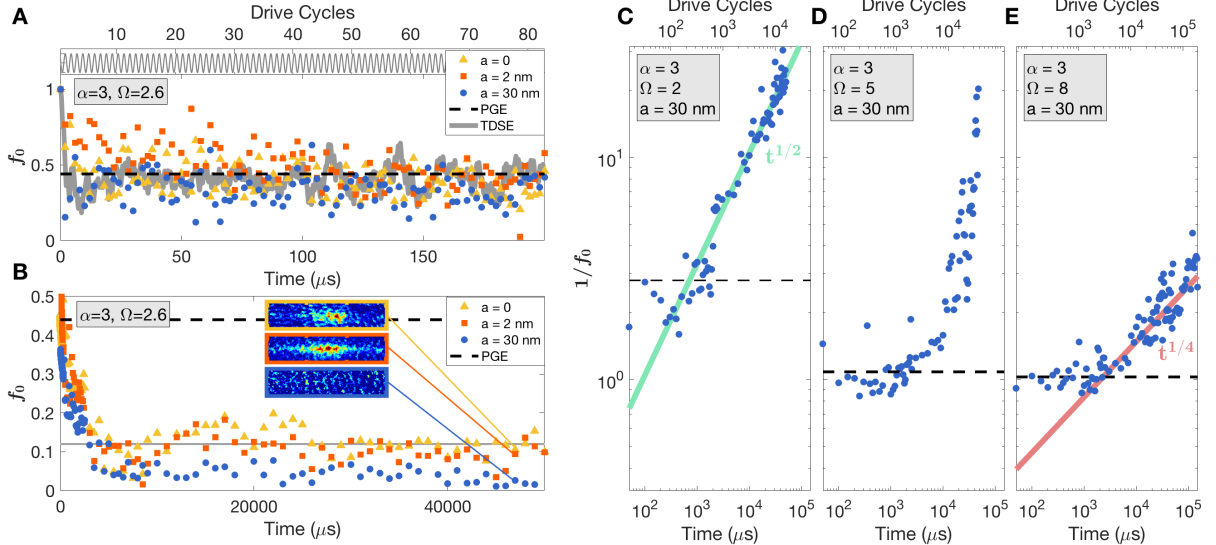


Figure 3: Interaction and frequency dependence of long-time dynamics. **A:** Short-time evolution of f_0 for a drive with $\Omega = 2.6$ and $\alpha = 3$, at three different values of the s-wave scattering length a . Regardless of interaction strength, f_0 oscillates near the PGE value (dashed line). Solid gray line shows the solution to the time-dependent Schrodinger equation for the non-interacting case. Top panel shows the driving waveform. **B:** f_0 as a function of time for much longer times, for the same drive and interaction parameters. Data are boxcar-averaged into 200μ s bins. The non-interacting and weakly-interacting samples attain a second plateau well below the PGE value, while the strongest-interacting sample decays to the infinite temperature state. Insets contain band-mapped absorption images at the indicated drive times, showing no significant ground-band occupation for the strongest-interacting sample. **C-E:** Evolution of the participation ratio $1/f_0$ for $a = 30$ nm, $\alpha = 3$, and varying drive frequency as indicated in the inset. Dashed line indicates the PGE prediction for the constant- f_0 plateau which emerges as the frequency increases. The time-dependence of heating away from the prethermal plateau is observed to be strongly Ω -dependent: at low frequency the participation ratio grows approximately as the square root of time (green solid line), while at the highest frequency the heating is consistent with a $t^{1/4}$ dependence (red solid line).

ratio $1/f_0$ for the strongest-interacting samples at various values of the drive frequency Ω . At $\Omega = 2$, $\alpha = 3$, the observed long-time evolution of $1/f_0$ is consistent with the \sqrt{t} dependence naively expected from Joule heating, and no significant plateau is observed. As the drive frequency is increased holding α constant, we observe the emergence of a quasi-static plateau lasting thousands of drive cycles, at a value of f_0 consistent with the PGE prediction. This plateau too eventually decays. Intriguingly, for the highest-frequency drives like the $\Omega = 8$ drive of Fig. 3E, the long-time departure from this second plateau is consistent with a $t^{1/4}$ time dependence, and is clearly slower than for the lower drive frequencies. This behavior

is consistent with the sub-Joule heating predicted by a recent theoretical analysis of a driven $O(N)$ model (27).

In conclusion, we have experimentally controlled and quantified prethermal localization in a many-body Floquet system. We observe Floquet prethermalization, a Floquet delocalization crossover which is in quantitative agreement with predictions of a theory based on the periodic Gibbs ensemble, and a long-time transition to ergodicity which depends strongly on drive frequency and interaction strength.

References

1. J. Zhang, *et al.*, *Nature* **543**, 217 (2017).
2. S. Choi, *et al.*, *Nature* **543**, 221 (2017).
3. R. Moessner, S. L. Sondhi, *Nat. Phys.* **13**, 424 EP (2017).
4. M. Holthaus, *Journal of Physics B: Atomic, Molecular and Optical Physics* **49**, 013001 (2016).
5. A. Eckardt, *Reviews of Modern Physics* **89**, 011004 (2017).
6. P. Roushan, *et al.*, *Nat. Phys.* **13**, 146 EP (2016).
7. N. Fläschner, *et al.*, *Science* **352**, 1091 (2016).
8. G. Jotzu, *et al.*, *Nature* **515**, 237 EP (2014).
9. M. Aidelsburger, *et al.*, *Nat. Phys.* **11**, 162 EP (2014).
10. M. C. Rechtsman, *et al.*, *Nature* **496**, 196 EP (2013).
11. K. M. Fujiwara, *et al.*, <https://arxiv.org/abs/1806.07858> (2018).
12. T. Mori, T. N. Ikeda, E. Kaminishi, M. Ueda, *Journal of Physics B: Atomic, Molecular and Optical Physics* **51**, 112001 (2018).
13. T. Kuwahara, T. Mori, K. Saito, *Annals of Physics* **367**, 96 (2016).
14. D. A. Abanin, W. De Roeck, F. Huveneers, *Phys. Rev. Lett.* **115**, 256803 (2015).
15. D. A. Abanin, W. De Roeck, W. W. Ho, F. Huveneers, *Phys. Rev. B* **95**, 014112 (2017).

16. F. Machado, G. D. Meyer, D. V. Else, C. Nayak, N. Y. Yao, <https://arxiv.org/abs/1708.01620> (2017).
17. J. Berges, S. Borsányi, C. Wetterich, *Physical Review Letters* **93**, 142002 (2004).
18. M. Moeckel, S. Kehrein, *Phys. Rev. Lett.* **100**, 175702 (2008).
19. M. Rigol, V. Dunjko, V. Yurovsky, M. Olshanii, *Physical Review Letters* **98**, 50404 (2007).
20. A. Polkovnikov, K. Sengupta, A. Silva, M. Vengalattore, *Rev. Mod. Phys.* **83**, 1 (2011).
21. M. Kollar, F. A. Wolf, M. Eckstein, *Phys. Rev. B* **84**, 054304 (2011).
22. M. Gring, *et al.*, *Science* **337**, 1318 (2012).
23. T. Langen, *et al.*, *Science* **348**, 207 (2015).
24. Y. Tang, *et al.*, *Phys. Rev. X* **8**, 021030 (2018).
25. A. Lazarides, A. Das, R. Moessner, *Phys. Rev. Lett.* **112**, 150401 (2014).
26. A. Lazarides, A. Das, R. Moessner, *Phys. Rev. E* **90**, 012110 (2014).
27. S. A. Weidinger, M. Knap, *Sci. Rep.* **7**, 45382 (2017).
28. E. Canovi, M. Kollar, M. Eckstein, *Phys. Rev. E* **93**, 012130 (2016).
29. M. Bükov, S. Gopalakrishnan, M. Knap, E. Demler, *Phys Rev Lett* **115**, 205301 (2015).
30. P. Bordia, H. Lüschen, U. Schneider, M. Knap, I. Bloch, *Nat. Phys.* **13**, 460 EP (2017).
31. M. Reitter, *et al.*, *Phys. Rev. Lett.* **119**, 200402 (2017).
32. M. Messer, *et al.*, <https://arxiv.org/abs/1808.00506> (2018).
33. J. Nager, *et al.*, <https://arxiv.org/abs/1808.07462> (2018).
34. M. Weinberg, *et al.*, *Phys. Rev. A* **92**, 043621 (2015).
35. D. McKay, M. White, B. DeMarco, *Phys. Rev. A* **79**, 063605 (2009).
36. A. Russomanno, A. Silva, G. E. Santoro, *Phys. Rev. Lett.* **109**, 257201 (2012).
37. L. D’Alessio, M. Rigol, *Phys. Rev. X* **4**, 041048 (2014).

Acknowledgments

The authors thank Jörg Schmiedmayer, Tarun Grover, Norman Yao, Chetan Nayak, Sid Parameswaran, Sarang Gopalakrishnan, Chaitanya Murthy, and Michael Knap for useful discussions, thank Sean Frazier for experimental assistance, and acknowledge support from the Army Research Office (PECASE W911NF1410154 and MURI W911NF1710323), the National Science Foundation (CAREER 1555313), the Office of Naval Research (N00014-14-1-0805 and N00014-16-1-2225), and the German Research Foundation (DFG) via the Research Unit FOR 2414 and the Gottfried Wilhelm Leibniz Prize program.

Supplementary Materials

Materials and Methods

Sample preparation and loading

The experiments begin with evaporation of bosonic ^7Li atoms in a crossed optical dipole trap ($\lambda=1064$ nm, 7 W per beam, $100\ \mu\text{m}$ beam waist, 1 kHz transverse trap frequencies) to generate a Bose-Einstein Condensate (BEC) with approximately 100,000 atoms at a temperature of 20 nK. During and after evaporation, the interatomic interaction strength is controlled by Feshbach tuning. We hold the BEC in the optical trap while ramping a homogeneous magnetic field from the value used for evaporation (729 G, $a \approx 30$ nm) to the desired final value in 100 ms. We then adiabatically load the atoms into the ground state of a combined 1D optical lattice with an initial static lattice depth of $V_0 = 10E_R$, where $E_R = \frac{\hbar^2 k_L^2}{2m}$ is the lattice recoil energy. In the static lattice, the tunneling rate between lattice sites is 483 Hz and the lattice site trap frequency is $\omega_0 = 159$ kHz. The transverse confinement is provided by the Gaussian lattice beams, resulting in a transverse trapping frequency of $449\ \text{Hz} \times \sqrt{1 + \alpha/2}$. We observe no significant excitation of transverse oscillator modes in the experiments reported here. Any additional forces along the lattice direction arising from magnetic field curvature or lattice beam intensity gradients are nulled out using magnetic shim coils to increase the period of Bloch oscillations to time scales significantly longer than our longest experiments. The interacting experiments are performed at Feshbach-induced s -wave scattering lengths of 2 nm and 30 nm, resulting in Thomas-Fermi interaction energies of 1.3 kHz and 3.8 kHz, respectively, for $\alpha = 0$. The Thomas-Fermi interaction energies grow with the modulation depth as $(\alpha + 2)^{\frac{2}{5}}$.

Optical lattice for sign-changing modulation

To enable realization of the $\alpha > 1$ regime of ultrastrong lattice modulation, a combined lattice is formed by overlapping two 1D optical lattices with a relative spatial phase shift of half a period. We use up to 7 W of 1064 nm light per beam and an $88\ \mu\text{m}$ beam waist. The two lattices are separated in frequency by 160 MHz, and have orthogonal linear polarizations. The beams are retroreflected by the same mirror to form two independent lattices. The relative phase is controlled by means of a waveplate stack, arranged so that the one of the lattices receives a $\lambda/4$ phase shift as it is retroreflected. This causes the two lattices to cancel each other when both beams have the same power, resulting in a featureless optical dipole trap; intentionally imbalancing the power results in a lattice of controllable sign. The depth of the combined lattice and the relative spatial phase between the two lattices are calibrated using matter-wave diffraction. After ramp-up of the combined lattice to an initial depth of $10 E_R$, the system is

quenched into the Floquet Hamiltonian by applying lattice amplitude modulation with some Ω and α . The amplitude of the combined lattice is modulated at up to 2 MHz by simultaneously varying the power of RF signals sent to two acousto-optical modulators from an AD9854 DDS board. Crucially, this double lattice modulation allows us to create a combined optical lattice that can change sign, where maxima (minima) become minima (maxima) during a drive cycle.

Measurement protocol

After the system is allowed to evolve for a fixed time, the modulation is quenched off and the combined lattice can either be snapped off or ramped off adiabatically with respect to the bandgaps to perform band-mapping (35). Resonant absorption imaging measures the atom number in the ground and excited bands. All band-mapping measurements are performed at a time-of-flight (TOF) of 1.25 ms. At this TOF, the initial Heisenberg-limited spatial distribution of the condensate is convolved with the momentum distribution, limiting our quasimomentum resolution to $\sim 0.2k_L$.

f_0 as an inverse participation ratio

A key point of this report is that f_0 provides a quantitative measure for localization and non-ergodicity. An intuitive picture for the relaxation of an isolated periodically-driven quantum system can be given as follows. The time dependent Schrödinger equation of the driven system possesses quasi-stationary solutions, called Floquet states, which are of the form $|n(t)\rangle e^{it\varepsilon_n/\hbar}$, with real quasienergy ε_n and time-periodic Floquet mode $|n(t)\rangle = |n(t+T)\rangle$, where $T = 2\pi/\omega$ denotes the driving period. For each time t they form an orthogonal basis, so that for a given pure initial state $|\psi(0)\rangle$ the evolved state can be expressed as $|\psi(t)\rangle = \sum_n c_n |n(t)\rangle e^{-i\varepsilon_n t/\hbar}$, with time-independent coefficients $c_n = \langle n(0)|\psi(0)\rangle$. Accordingly, expectation values of observables \hat{O} evolve like $\langle \hat{O}(t) \rangle = \sum_{nn'} c_n^* c_{n'} \langle n(t)|\hat{O}|n'(t)\rangle e^{it(\varepsilon_n - \varepsilon_{n'})/\hbar}$. The relaxation to a quasi-steady state (i.e. a time-periodic state) in the long-time limit can be associated with the dephasing and averaging out of the off-diagonal terms, so that asymptotically $\langle \hat{O}(t) \rangle \simeq \sum_n |c_n|^2 \langle n(t)|\hat{O}|n(t)\rangle$, corresponding to a Floquet diagonal ensemble described by a periodic density operator $\hat{\rho}_{\text{dia}}(t) = \sum_n |c_n|^2 |n(t)\rangle \langle n(t)|$ (36). While in a many-body system, the diagonal ensemble is still characterized by an exponentially large number of probabilities $|c_n|^2$, it is believed that the quasi-steady state is characterized by a periodic Gibbs ensemble (PGE), $\rho_{\text{PGE}}(t) = Z^{-1} \exp[-\sum_j \lambda_j \hat{I}_j(t)]$, with $\hat{I}_j(t) = \hat{I}_j(t+T)$ denoting the integrals of motion of the system (25). For the non-interacting driven gas, we have an extensive number of integrals of motion given by the number operators $\hat{n}_j(t)$ of the single-particle Floquet modes $|j(t)\rangle = |j(t+T)\rangle$. The expectation values of these operators determine the PGE so that the system is non-ergodic (i.e. localized). A generic interacting Floquet system should at sufficiently

long times approach a fully ergodic infinite-temperature state $\rho_{\text{ergodic}} \propto 1$ (26, 37). However, even the interacting system can approach a prethermal state that is accurately described by the PGE on intermediate, and potentially exponentially long, time scales.

To quantify the degree of localization (non-ergodicity), we initially prepare the system in the undriven ground-state $|\psi_0\rangle$, so that $c_n = \langle n(0)|\psi_0\rangle$, and consider the expectation value of the projector $\hat{O} = |\psi_0\rangle\langle\psi_0|$ at stroboscopic times $t_\nu = \nu T$ with integer ν , which is equal to the squared overlap $|\langle\psi_0|\psi(t_\nu)\rangle|^2$ with the evolved state $|\psi(t_\nu)\rangle$. According to the diagonal ensemble and employing $|n(t_\nu)\rangle = |n(0)\rangle$, the long-time average (indicated by an overbar) over the stroboscopic dynamics of this quantity gives

$$\overline{|\langle\psi_0|\psi(t_\nu)\rangle|^2} = \sum_n |\langle\psi_0|n(0)\rangle|^4 \equiv \text{IPR}. \quad (1)$$

This quantity directly corresponds to the inverse participation ratio that quantifies the localization of the ground state $|\psi_0\rangle$ in the basis of the Floquet states. Its inverse, $1/\text{IPR}$, is a direct measure for the number of Floquet states required to represent $|\psi_0\rangle$. For the non-interacting gas, we find that the desired overlap is given by the fraction of atoms populating the single-particle ground state (i.e. the quasimomentum $k = 0$ mode in the lowest Bloch band), $|\langle\psi_0|\psi(t_\nu)\rangle|^2 = f_0(t_\nu)$, which we have measured for example in Fig. 1B. Thus, having relaxed to a quasi-steady state, we have

$$\text{IPR} = \overline{f_0(t_\nu)}, \quad (2)$$

so that the measured observable directly quantifies non-ergodicity. For the interacting system, this reasoning can still be applied in the prethermal regime.

Supplementary Text

Approach to the PGE quasi-steady state

The PGE quasi-steady state is expected to be rapidly established after the initial quench (25). At any point in drive parameter space, we can measure the approach to the PGE state by observing the full time evolution during the drive. As shown in Fig. S1A, band-mapping (35) at variable drive time shows a near-immediate approach to the value of f_0 predicted by theory, on a timescale similar to the drive period. The rapid but not instantaneous nature of the dephasing responsible for the emergence of the prethermal plateau can be revealed by measuring a different observable: the interference patterns after the system is quenched back to a static lattice which is snapped off immediately rather than band-mapped. Fig. S1B shows that over the course of a few dozen drive cycles, the occupations of the first 2 interference peaks approach their quasi-steady-state values.

Finite Band Occupation

Here we briefly discuss the reason that only a finite number of bands are expected to be significantly occupied. Since quasimomentum is conserved in the absence of interactions, the single-particle Hamiltonian H of the system can be expressed in terms of states $|m\rangle$ having momentum wave numbers $K_m = (4\pi/\lambda)m$ for integer m . In units of the recoil energy E_R ,

$$H = 4 \sum_m \left[m^2 |m\rangle\langle m| + \frac{V(t)}{16} \left(|m+1\rangle\langle m| + |m-1\rangle\langle m| \right) \right] \quad (3)$$

with $V(t) = (V_0/E_R)[1 + \alpha \cos(\omega t)]$. Thus, already for $|m| \simeq 1$, the energy separation $(m+1)^2 - m^2 = 2m+1$ to higher-lying states becomes larger than the time-dependent coupling matrix elements $V(t)/16$ and the driving frequency. This suggests that the drive will cause substantial redistribution among small m , while for large m the Floquet states will not significantly differ from the undriven eigenstates of the system at large m that correspond to the scattering continuum. In other words, the ground state of the non-interacting system will mainly overlap with a few Floquet states. The Hamiltonian (3) explains also the origin of the crossover to a highly localized regime with f_0 close to one for large frequencies as we observe it in Fig. 1. The fact that it couples only neighboring momenta m and $m \pm 1$ shows that (except for narrow resonances) the ground state is predominantly coupled to low energy states, transitions to which become off resonant for large drive frequencies.

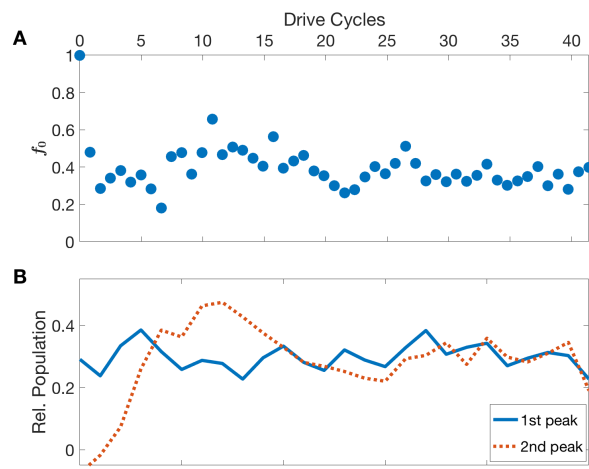


Figure S1: Entering the prethermal state. **A:** Normalized ground band occupation f_0 as a function of time during modulation with $\alpha = 3$, $\Omega = 2.6$, $a = 0$. The system attains the prethermal value of f_0 on time scales comparable to a single drive cycle. **B:** Population fraction in diffracted peaks after diabatic lattice snapoff, as a function of time during the same drive. Gradual attainment of the prethermal steady-state is apparent in the increase and settling of the second-peak population.